J. Appl. Environ. Biol. Sci., 4(6)72-79, 2014

ISSN: 2090-4274
Journal of Applied Environmental and Biological Sciences
www.textroad.com

Numerical Simulation of Barricades under Blast Wave Propagation

Mohammad Aghaei Asl[1], Kambiz Kangarlou*[2]

[1]Assistant Professor, Department of Civil Engineering, Payame Noor University of Tabriz, Iran
[2]Postdoctoral Researcher, Biomedical Engineering Department, Amir Kabir University of Technology, Tehran, Iran

Received: April 22, 2014
Accepted: June 11, 2014

ABSTRACT

Barricade is one of the most efficient means available to protect persons, goods and facilities against fragments. It is also an efficient solution to minimize blast hazards by reducing overpressure level just behind.
Purpose of this study is to check that there is effectively an overpressure decrease behind barricade and to assess it. Finite element (FE) modeling was carried out with a two dimensional finite volume code based on Euler equations. Numerical simulations and theoretical studies have been conducted to define how to design protection barriers that limit the propagation of blast waves in an explosion and to assess the ability of these barriers to reduce the harmful consequences of an explosion.
The insights gained from this research will be presented in a methodological guide for the practical use of physical protection barriers.

KEYWORDS: barricades, CFD modeling, blast wave, Euler equations, design protection.

INTRODUCTION

A barricade is a construction feature used to provide for safety in the design of explosive facilities. It is a natural or artificial terrain feature partially or totally surrounding a building and is intended to reduce the effects of an accidental explosion on other buildings. Some protection is considered to be provided by a natural or man-made hill, by another structure, or sometimes by trees. In military manuals for the construction of explosives facilities, a barricade is more precisely defined as a massive wall or mound of given dimensions and materials (Figure 1).

In general, these manuals provide for safety at explosives facilities by requiring specific spacing of other structures and facilities from a given quantity of explosives. The manuals require distances to be approximately doubled when neither the source nor the target building is barricaded. At facilities of the Department of Defense where large quantities of explosives are handled and stored, the use of barricades may require the expenditure of large sums of money, may involve the safety of many people, and may influence the acquisition of large land areas. It is therefore essential that the Armed Services have available the best possible information upon which to base the design of facilities for storing, transporting, and handling of ammunition and other explosives.[1]

(a) **(b)** **(c)**

Figure 1: (a) The First World War (http://arw.ir), (b) Earthen barricade during the Warsaw Uprising (http://en.wikipedia.org/wiki/Barricade), (c) U.S. forces on the border of Afghanistan and Pakistan (http://www.taknaz.ir).

***Corresponding Author:** Dr.Kambiz Kangarlou, Postdoctoral Researcher, Biomedical Engineering Department, Amir Kabir University of Technology, Tehran, Iran. Email: kangarloo_kambiz@yahoo.com

In the case of pressure waves resulting from an explosion, the establishment of physical protection barriers would reduce the effects of distance (and thus the extent of the exclusion zone around the facility), the potential damage to individuals and property, and thus the cost of a risk prevention policy for hazardous installations. This technique is used in the control of major risks and more severe scenarios in particular. If the implementation of these barriers (which significantly limits their use) is not more fully understood and their design criteria are not so well established, then such measures could not be recommended for a variety of industrial sites. The existing literature has shown that a physical protection barrier can effectively reduce the rate of loading by a blast wave and can protect structures when they are close to the screen. However, the effect of these barriers has not yet been quantified for various types of explosions and barrier geometries, and the scope of this protection downstream of the barrier has not been established. This lack of quantification is the reason for which the existing literature has not proposed an analytical expression characterizing the effect of a blast wave on the structures behind a protective physical barrier or determined the generic sizing of a barrier.[2]

MATERIALS AND METHODS

Blast wave phenomena.

The violent release of energy from a detonation in a gaseous medium gives a sudden pressure increase in that medium. The pressure disturbance, termed the blast wave, is characterized by an almost instantaneous rise from the ambient pressure to a peak incident pressure (P_{pos}).[3, 4] This pressure increase, or shock front, travels radially from the burst point with a diminishing velocity that always is in excess of the sonic velocity of the medium. Gas molecules making up the front move at lower velocities. This latter particle velocity is associated with a "dynamic pressure," or the pressure formed by the winds produced by the shock front.[5]

Friedlander described a typical pressure-time profile of an explosion in a free field, i.e. without reactions.[6] This curve is depicted in Figure 2.

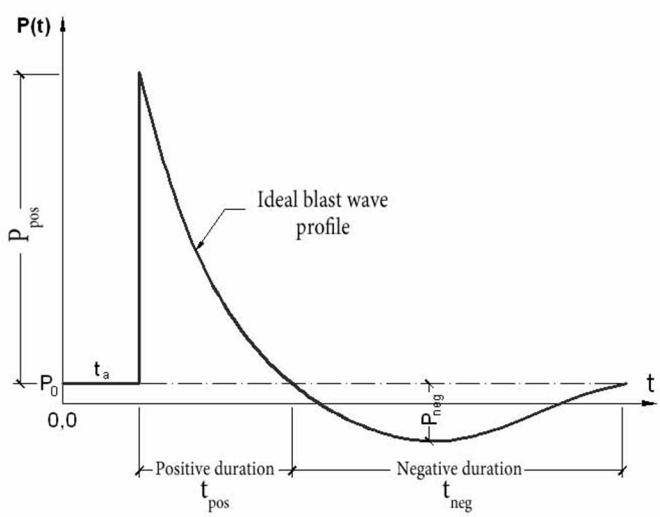

Figure 2: Ideal blast wave profile vs. time relation at a fixed point as defined by the biphasic Friendlander equation.[6]

The pressure-time history of a spherical blast can be expressed in the form of the Friedlander equation, based on the Sedov-Taylor blast wave solution:[7]

$$P(t) = P_0 + \left(P_{pos} - P_0\right)\left[1 - \frac{(t - t_a)}{t_{pos}}\right] e^{-b\frac{(t-t_a)}{t_{pos}}} \quad (1)$$

The parameter, b describes the decay of the curve, P_0 is the ambient air pressure and t_a is the time at peak positive over pressure. Recently, Teich and Gebekken[8] proposed a new formula to compute the wave decay parameter, $b=1.5Z^{-0.38}$ ($01<Z<30$) and based on Larcher[9] work, $b=5.2777Z^{-1.1975}$. The equations 2-10 were presented to compute peak positive over pressure (P_{pos}) variation with scaled distance (z), the positive phase of duration (t_{pos}) and the positive impulse (I_{pos}).

Henrych based on the analysis of several experimental data:[10]

$$P_{pos} = \begin{cases} \frac{14.072}{Z} + \frac{5.540}{Z^2} - \frac{0.357}{Z^3} + \frac{0.00625}{Z^4} (bar) & (0.05 < z < 0.3) \\ \frac{6.194}{z} - \frac{0.326}{z^2} + \frac{2.132}{z^3} (bar) & (0.3 < z < 1) \\ \frac{0.662}{z} + \frac{4.05}{z^2} + \frac{3.228}{z^3} (bar) & (1 < z < 10) \end{cases} \quad (2)$$

$$t_{pos} = e^{(-2.75+0.27logZ)+logW^{1/3}} (mS) \quad (3)$$

Kinney and Grahm based on the analysis of large experimental data:[11]

$$P_{pos} = P_0 \frac{808\left[1+\left(\frac{Z}{4.5}\right)^2\right]}{\sqrt{\left[1+\left(\frac{Z}{0.048}\right)^2\right]} \times \sqrt{\left[1+\left(\frac{Z}{0.32}\right)^2\right]} \times \sqrt{\left[1+\left(\frac{Z}{1.35}\right)^2\right]}} (bar) \quad (4)$$

$$t_{pos} = W^{1/3} \frac{980\left[1+\left(\frac{Z}{0.54}\right)^{10}\right]}{\left[1+\left(\frac{Z}{0.02}\right)^3\right] \times \left[1+\left(\frac{Z}{0.74}\right)^6\right] \times \sqrt{\left[1+\left(\frac{Z}{6.9}\right)^2\right]}} (milisecond) \quad (5)$$

$$I_{pos} = \frac{0.067\sqrt{1+\left(\frac{Z}{0.23}\right)^4}}{Z^2\sqrt[3]{1+\left(\frac{Z}{1.55}\right)^3}} (bar-ms) \quad (6)$$

Sadovskiy, based on explosion data analysis:[12]

$$P_{pos} = 0.085\frac{W^{1/3}}{R} + 0.3\left(\frac{W^{1/3}}{R}\right)^2 + 0.8\left(\frac{W^{1/3}}{R}\right)^3 (MPa) \quad (7)$$

$$t_{pos} = 1.2\sqrt[6]{W}\sqrt{R}\,(ms) \quad (8)$$

$$I_{pos} = 200\frac{W^{2/3}}{R} (Pa-s) \quad (9)$$

Where W is the charge weight in kg, Z is the scaled distance in m and expressed as:

$$Z = \frac{R}{W^{1/3}} (m/kg^{1/3}), \quad R_2 = R_1\left(\frac{W_2}{W_1}\right)^{1/3} \quad (10)$$

FE models of explosive in free air

Finite element analysis was performed using Ansys 3D. The complete definition of a transient non-linear dynamics problem (such as the interactions of blast waves with the barricades) entails the knowledge of the material models that define the relationships between the variables pressure, mass-density, energy-density, temperature, etc. These relations typically involve an equation of state (EOS), a strength model and a failure model for each constituent material.

Modeling of the explosive. The detonation and expansion of the TNT explosive materials was described using the JWL (Jones-Wilkins-Lee) equation of state (EOS) along with a high explosive material definition. The JWL equation is described as:

$$p_{EOS} = A\left(1-\frac{\omega}{R_1V}\right)e^{-R_1V} + B\left(1-\frac{\omega}{R_2V}\right)e^{-R_2V} + \omega\frac{E_0}{V} \quad (11)$$

Where $V = \rho_0$ (initial density of an explosive)/ρ (density of detonation gas). E_0 is specific internal Energy per unit mass. A, B, R_1, R_2, ω are JWL fitting parameters. The parameters for the JWL equation can be found, for example, in Dobratz and Crawford.[13] The values used for TNT explosives are shown in table 1.

Table 1. JWL and material parameters for TNT explosive.[13]

ρ_0 (kg/mm^3)	V (m/s)	A	B	R_1	R_2	ω	E_0 (GPa)
0.63e-6	6930	374	3.21	4.15	0.95	0.3	7

Key: ρ_0, initial density of an explosive; V, Detonation velocity; E_0, specific internal energy per unit mass; A, B, R_1, R_2, ω are Material constant (GPa).

Air material model. As mentioned earlier, the Eulerian domain was filled with air. Air was modeled as an ideal gas and, consequently, its EOS was defined by the ideal-gas gamma-law relation as:

$$P = (\gamma - 1)\frac{\rho}{\rho_0}E \qquad (12)$$

Where P is the pressure, γ the constant-pressure to constant-volume specific heats ratio (1.4 for a diatomic gas like air), ρ_0 (1.225 kg/m^3) the initial air mass density, and ρ the current density. For equation (12) to yield the standard atmosphere pressure of 101.3 kPa, the internal volumetric energy density E was set at 253.4 kJ/m^3, which corresponds to the air mass specific heat of 717.6 J/kg-K and a reference temperature of 290 K.

Determination of barricade model

Numerecal simulations of blast wave were performed with a CFD code based on the 3D compressive Euler equation. The calculation domain was 22m × 20m in X, Y and Z directions. In table 2 summarises the barrier configurations studied here. The dimensions are in accordance with the recommendations of NATO [14] and the frame thresholds.

Table 2. Dimensions of the barriers considered in this study.

Barrier	1	2	3	4	5	6
Height (m)	0.19	0.19	0.16	0.19	0.19	0.19
Thickness at the top (m)	0.03	0.03	0.06	0.19	0.19	0.19
Length (m)	0.80	0.40	0.80	1.30	1.30	0.40
Downstream angle α_1	45	45	45	45	90	90
Upstream angle α_2	45	45	45	90	45	45

RESULTS

An example plot of static pressure and velocity contour profile at the end of the run for barrier number 2 were shown in Figure 3 and 4. The barrier was subjected to an equivalent TNT value of 250 kg (547 lb) explosive charge at a stand-off distance of 10 m (33 ft).

When an explosion from a high explosive source occurs within a structure, blast waves will be reflected from the inner surfaces of the structure and imploded towards the center. The amplitude of the re-reflected waves will decay with each reflection and eventually the pressure will settle to an ambient pressure. In the calculation the load was applied to the walls with an air blast in which the pressure varies from element to element. The pressure applied was stored in a data array containing a range of the element and the corresponding pressure value. In order to apply a uniform pressure, the range and the explosive incidence angle were explicitly set so that all surfaces were loaded with the same value of pressure.

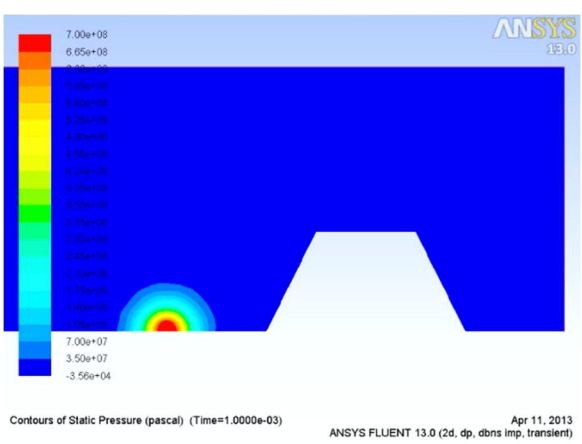

time: 1 (ms)

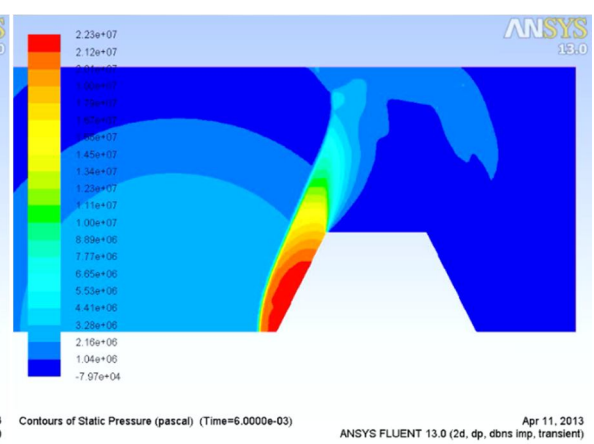

time: 6 (ms)

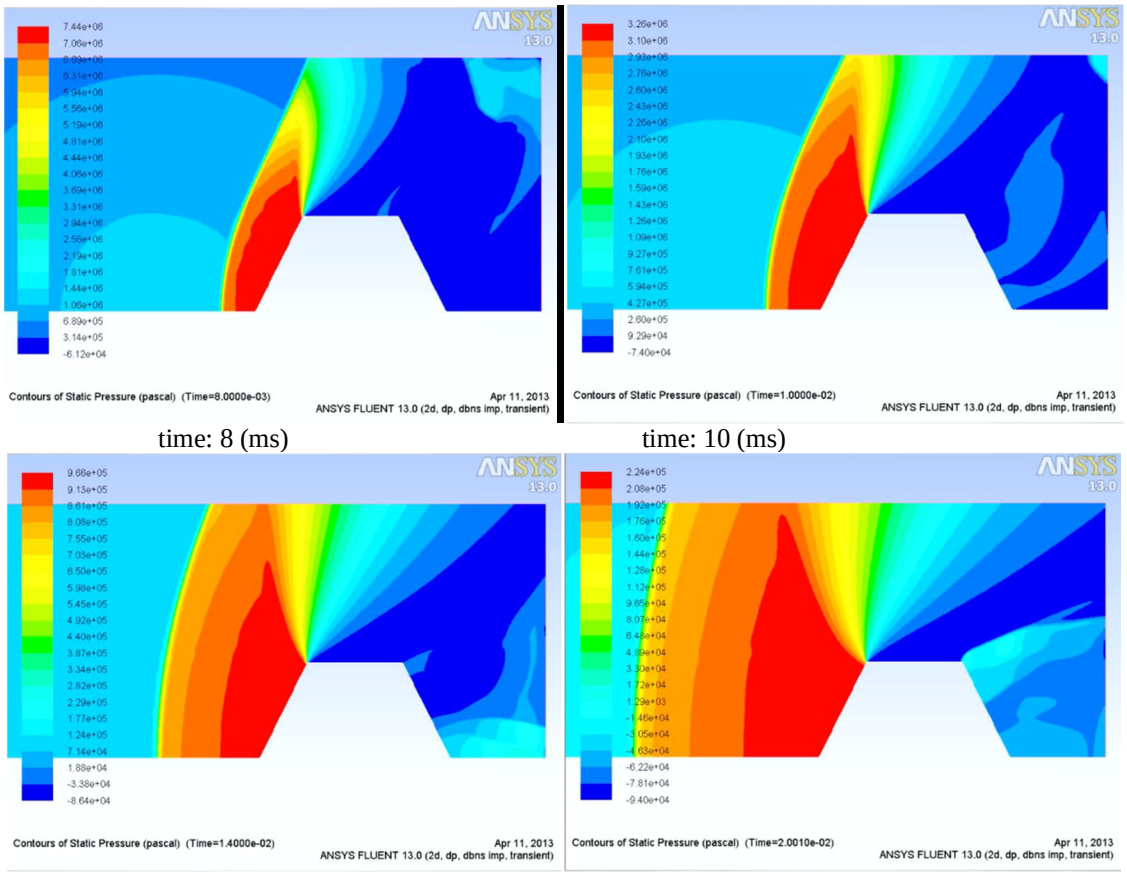

time: 8 (ms) time: 10 (ms)

time: 14 (ms) time: 20 (ms)

Figure 3: Static pressure contours at various time steps in the detonation case 2.

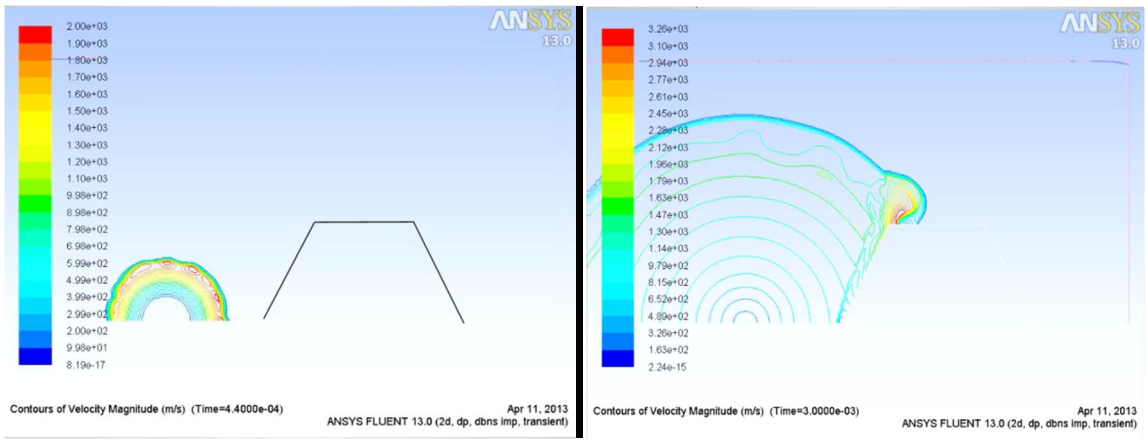

time: 0.44 (ms) time: 3 (ms)

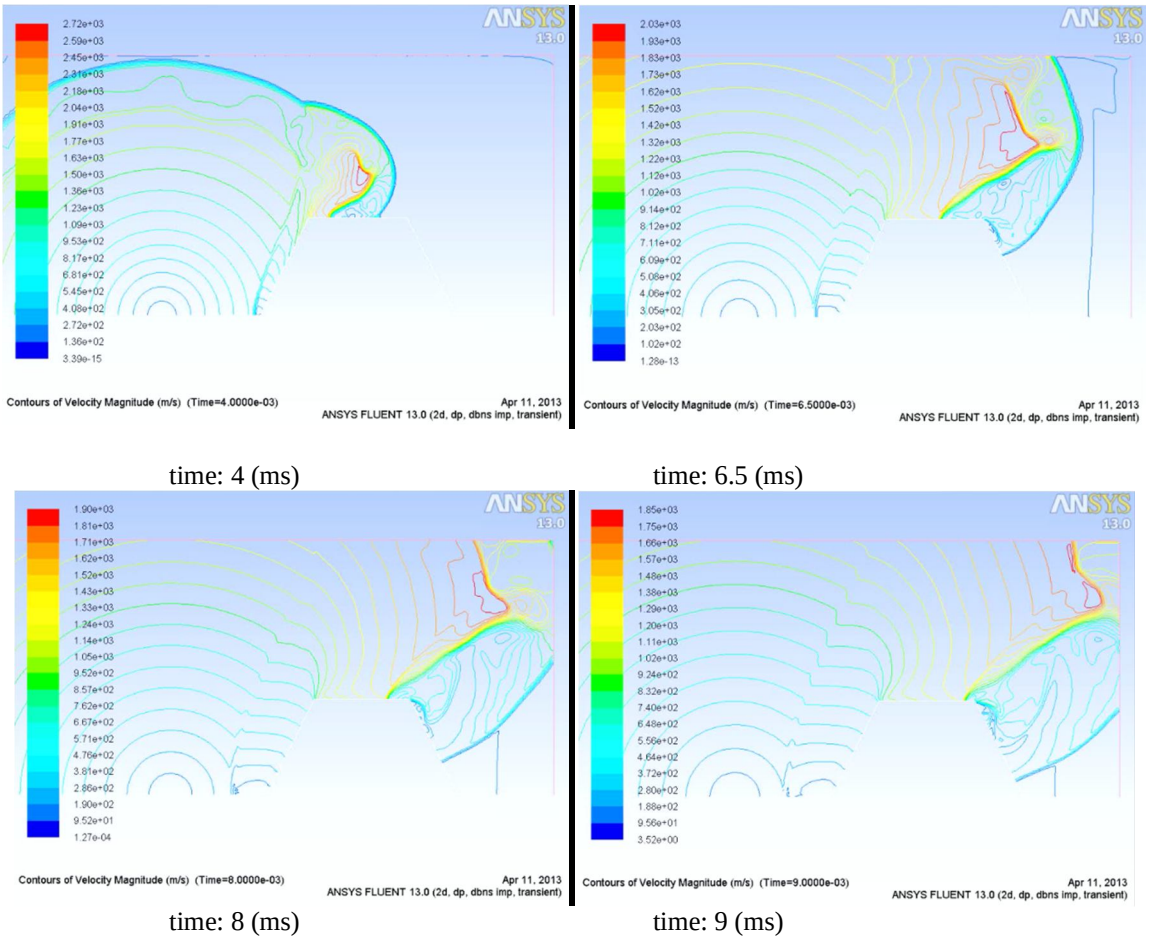

time: 4 (ms) time: 6.5 (ms)

time: 8 (ms) time: 9 (ms)

Figure 4: The velocity contours at various time steps in the detonation case 2.

DISCUSSION

The phenomena analysis was conducted from the simulations validated experimentally. This analysis can be described in the three steps of propagation of the shock wave: 1- on the upstream side, 2- on the top and 3- on the downstream face and downstream of the barrier. The incident shock wave generated by the detonation of the charge gas impacts the upstream side of the barrier and is reflected. Reflection of the incident wave can be regular or Mach. The reflected wave propagates in a medium composed of two zones, the burned gases (detonation products) and air. At the interface between these two zones, a wave is transmitted in the burned gases and another is transmitted in the air. The latter catches the incident shock wave and results in recombination around the wave reflected on the original interface. The detonation products create increased pressure and impulse on the upstream side of the barrier. A critical distance can be determined based on the geometry of the barrier, the nature of the explosive charge and its mass.[2] Rarefaction waves occur at the top of the barrier. The greater the thickness of the top of the barrier, the more important the effect of relaxation is in reducing the pressure. Furthermore, a second expansion occurs on the downstream corner of the top of the barrier. Relaxation then continues on the downstream face. The wave arriving at the base of the barrier continues to propagate and is reflected on the ground. The amplitude of the reflected wave and the nature of the reflection depend on the history of the wave and the geometry of the downstream barrier. In the case of a small barrier (Length < 0.4 m), the waves from the side faces are combined with that from the top, leading to the formation of a Mach stem and an increase in pressure downstream of the barrier.[2]

The experimental work of Allain (1994) and the numerical studies of Borgers (2010) have obtained different findings for this type of structure without a thickness at the top (e = 0 m) and with one or two 45- degree slopes. These studies have shown that the reflection on the upstream side (facing the explosion) can be regular or Mach is followed by rarefaction waves, the reflection is continued on the downstream face (rear), which accelerates the front

and the reflection on the ground, thus increasing the pressure. The evolution of the pressure throughout the propagation of the shock wave does not obey a linear function in terms of the distance from the centre of the explosive charge. Therefore, the protective effects of the barrier are dependent on its geometry (e.g., length and thickness at the top corners of the upstream and downstream sides).
NATO AC 258 [14] has introduced a few years ago "Quantity Distance" notion to ensure the minimum practicable risk to life and property. French Regulation 2 kept also this concept by defining five hazardous areas depending on level of potential damages on personal and property (Table 3).

Table 3. Hazardous areas definition.[14, 15]

	Z1	Z21	Z3	Z4	Z51
Foreseeable personal injury	**Lethal injury in more than 50% of cases**	**Serious injuries Which may be lethal**	**injuries**	**Possibility of injuries**	**Very low possibility of slight injuries**
Foreseeable property damage	Very serious damage	Serious damage	Medium and slight damage	Slight damage	Very slight damage

As we can notice on this table, definitions are rather qualitative than quantitative. However, hazardous areas limits are determined with simple formula. For example, hazard division products (mass exploding) radius of circular concentric zone is given by:[15] $R = k\ Q^{1/3}$

Where k - coefficient depending on zone to be considered ($m/kg^{1/3}$), Q - net explosive quantity (kg) and R - radius of zone (m). Charge is supposed to be on the floor, in free field. More precisely, we have the following relationships: $R1 = 5\ Q^{1/3}$, $R2 = 8\ Q^{1/3}$, $R3 = 15\ Q^{1/3}$, $R4 = 22\ Q^{1/3}$, $R5 = 44\ Q^{1/3}$.

CONCLUSIONS

This analysis shows that the design of the barrier and its location upstream of the explosive charge depends on the area to be protected (immediately downstream at the base or further downstream of the barrier). In general, the configurations considered here indicate that the protective effect is greater when the barrier is close to the load and correspond with the findings of Allain[16] and Borgers[17]. The NATO recommendations did not specify the angles of the barrier or the distance between the charge and barrier. The results obtained by numerical simulations in 2-D asymmetric geometry (parametric study) for a charge of TNT were used to shed light on the evolution of the maximum overpressure and positive impulse at the ground and at a man's height.[2]

The objective of this research is to advance our understanding of the propagation of pressure waves from an external explosion (accidental or intentional) around a physical barrier protection.

This study aims to understand the physical phenomena of blast wave propagation around a physical protection barrier (propagation of waves arriving at a barrier face and bypassing the edges and top of the barrier, wave reflection due to buildings behind the screens) to define a guide for the geometric design of such barriers. Then, the ability of the designed barriers to reduce the effects of a blast wave resulting from a downstream explosion or detonation is evaluated.

REFERENCES

1. Filler WS, Rossi JM, Walsh RJ. *Barricade effectiveness evaluated from records of accidental explosions.* Armed Services Explosives Safety Board Washington D C, 1966.
2. Sochet I, Eveillard S, Piserchia PF, Vincont JY. *Dimensioning physical protection barricades against the propagation of pressure waves following a detonation*. Concepts, Systèmes et Outils pour la Sécurité Globale (CSOSG) projet BARPPRO, 2010.
3. Nyein MK. Computational modeling of blast-induced traumatic brain injury [thesis]. Cambridge, USA: Massachusetts Institute of Technology, 2010.
4. Elder GA, Dorr NP, De Gasperi R, Gama Sosa MA, Shaughness MC, Maudlin-Jeronimo E, Hall AA, McCarron RM, Ahlers ST. Blast exposure induces post-traumatic stress disorder-related traits in a rat model of mild traumatic brain injury. *J Neurotrauma*. 2012,29(16):2564-75. DOI: 10.1089/neu.2012.2510.
5. Elsayed NM, James Atkins JL. *Explosion and blast-related injuries: effects of explosion and blast from military operations and acts of terrorism*. Elsevier Academic Press,2008.
6. Goel MD, Matsagar VA, Gupta AK, Marburg IS. An Abridged Review of Blast Wave Parameters. *Defence Science Journal*. 2012,62(5):300-306.
7. Sedov LI. Propagation of strong shock waves. *J. App. Math. Mech*. 1946;10:241-50.

8. Teich M, Gebbeken N. The Influence of the under pressure phase on the dynamic response of structures subjected to blast loads. *Int. J. Prot. Str*. 2010,1(2):219-34.
9. Larcher M, Herrmann N, Stempniewski L. Explosions simulation leichter Hallenhüllkonstruktionen. *Bauingenieur*. 2006,81(6):271-77.
10. Henrych J. *The dynamics of explosion and its use*. Elsevier, Amsterdam,1979.
11. Kinney GF, Grahm KJ. *Explosive shocks in air*. Springer, Berlin,1985.
12. Sadovskiy MA. *Mechanical effects of air shockwaves from explosions according to experiments. In Sadovskiy M.A. Selected works: Geophysics and physics of explosion*. Nauka Press, Moscow,2004.
13. Dobratz BM, Crawford PC. *LLNL Explosives Handbook: Properties of Chemical Explosives and Explosive Simulants, Tech. Rep*. University of California; Lawrence Livermore National Laboratory. Report UCRL-5299; Rev.2,1985.
14. NATO AC/258 - D/425 (AASTP-1), May 1992.
15. Allain L. *Barricade influence on blast wave propagation*. SNPE Centre De Recherches Du Bouchet Vert-Le-Petit France, Aug1994.
16. Allain L. *Barricade influence on blast wave propagation*. SNPE / Division Defense and Space, private communication, 1994.
17. Borgers J. *Blast walls reviewed*. 21st Military Aspect of Blast and Shock (MABS), Jerusalem, October 4-8th 2010.